Kr spectra from an electron-beam ion trap: 300 nm to 460 nm

F. G. Serpa,* E. W. Bell,† E. S. Meyer,‡ J. D. Gillaspy, and J. R. Roberts
Atomic Physics Division, National Institute of Standards and Technology, Gaithersburg, Maryland 20899
(Received 9 October 1996)

Kr spectra from 300 nm to 460 nm produced in an electron-beam ion trap (EBIT) are reported in this work. The spectra include magnetic dipole ($M1$) transitions from Kr XXIII and Kr XXII, as well as electric dipole ($E1$) lines of Kr II and Kr III. Two new capabilities of the EBIT at the National Institute of Standards and Technology, time resolved data acquisition and extracted ion analysis, are used to aid in the charge state identification. [S1050-2947(97)03503-8]

PACS number(s): 32.30.Jc, 32.10.−f, 31.25.Eb, 31.25.Jf

I. INTRODUCTION

Recent developments in electron beam ion trap (EBIT) spectroscopy have shown the importance of the EBIT as a source of magnetic dipole ($M1$) transitions in the visible or near-uv [1,2]. Magnetic dipole transitions arising between levels of the ground configuration of highly charged ions are not only useful as diagnostic tools for tokamaks [3–5] and in the study of the solar corona [6,7], but also have academic interest since *ab initio* calculations fail to account for the observed wavelengths [5,8]. Many such transitions remain unobserved, particularly for charge states with ionization energies below 2 keV [9]. Measurements of such lines are important because they make significant impact on the elaboration of spectral [10] and energy level [11] databases. They are also important for improving predictions along isoelectronic sequences [9] and provide a challenge for *ab initio* calculations.

In the present work we report spectra from 300 nm to 460 nm obtained with the EBIT during injection of Kr gas. Our data include two $M1$ transitions, one of which has not been previously observed. These $M1$ lines arise from transitions between the levels of the ground configuration of Kr XXIII ($3s^2 3p^2$) and Kr XXII ($3s^2 3p^3$). A new ion extraction, transport, and charge-to-mass analysis system at the National Institute of Standards and Technology (NIST) [12] was used to obtain information about the distribution of ion charge states within the EBIT. Data from the extraction system together with time resolved data were used to aid in charge state identification. Lines of singly and doubly ionized Kr were also present in our spectra and were used for *in situ* wavelength calibration.

II. EXPERIMENTAL SETUP

The EBIT at NIST was used as the source of excited highly charged ions in this work [13,14]. The desired ion stage is produced by successive electron-impact ionization from an accelerated electron beam, produced by a electron gun which provides currents up to ~150 mA. A pair of superconducting magnets in a Helmholtz configuration produces an axial magnetic field of 3 T in the trap region and compresses the electron beam to a diameter of ~60 μm, resulting in a current density of ~5000 A/cm^2. Together the electron beam and the magnetic field produce a radial trap for the ions. Axial trapping of the ions along the electron beam axis is provided by raising the two ends of three collinear, insulated drift tubes to a positive potential with respect to the center drift tube bias potential. Together this traps a cylindrical ion cloud ~30 mm long and ~200 μm in diameter [15], oriented along the direction of the electron beam. A variable bias voltage from 2 kV to 20 kV is applied to the drift tubes to define an accelerating potential for the electron beam. A correction of approximately −100 eV must be applied to this energy in order to account for the net space charge of the electrons and the positive ions in the trap in this particular experiment. The precise energy of the electron beam (~50 eV width) is determined from the accelerating bias potential, the center drift tube floating voltage, and the space charge correction. By adjusting the accelerating voltage slightly below the ionization energy of the desired ion, the relative population of a specific charge state can be optimized.

A gas injection system connected to a lateral port, that looks directly into the trap, is used to introduce krypton atoms into the EBIT from a direction perpendicular to the trap. The gas injection system consists of a tunable gas leak, two pump chambers, and three collinear apertures. The apertures are used to define the differential pumping of the chambers and for rough alignment of the gas stream. The first aperture (0.318 cm in diameter) is located 67.7 cm from the trap and separates the gas leak from the first chamber. The second aperture (1.27 cm diameter) is located 44.5 cm from the trap and separates the first and second chambers. The last aperture (0.318 cm diameter) is located 32.1 cm from the trap and separates the second chamber and the injection port to the EBIT. The gas leak allows for tuning of the amount of gas injected, which is monitored by an ion gauge located in the chamber between the first and second apertures. Typical gas injection pressure values for this experiment were $\sim 5\times10^{-4}$ Pa to $\sim 2\times10^{-3}$ Pa. Each chamber is pumped by a turbo pump with a pumping speed of about 50 l/sec.

*Permanent address: Physics Department, University of Notre Dame, Notre Dame, IN 46556.
†Present address: Diamond Semiconductor Group, 14 Blackburn Center, Gloucester, MA 01930.
‡Permanent address: D.E. Shaw Co., 120 West 45th, New York, NY 10036.

The detection system is described in detail elsewhere [1,2]. Briefly, a cooled, low noise photomultiplier was used for photon detection, and a scanning monochromator was used for wavelength selection. Radiation emanating from the trap was imaged onto the entrance slits of the scanning monochromator using a set of two plano-convex lenses; this was necessary to keep the photomultiplier away from any stray magnetic field from the superconducting magnet and to improve the signal. The entire optical table which supports the monochromator was attached to two perpendicular translation stages which can be positioned with a resolution better than 10 μm. These translation stages were used to place the monochromator's entrance slit at the image of the trap produced by the lens system.

The trap was emptied of ions at preset time intervals by sending a fast pulse to the middle drift tube. This pulse raised the middle drift tube floating voltage above the upper and lower drift tube floating voltages in less than 1 ms, kept it constant for $\sim$0.1 ms, and lowered it back to its initial value again in less than 1 ms, so that the total duration of the pulse was less than 2 ms. Time resolved data were acquired by setting the monochromator to a particular wavelength and accumulating data over thousands of such cycles. Photons arriving at the photomultiplier were time-stamped with a resolution better than 0.1 ms. The timing electronics were designed using CAMAC modules controlled by a list processor interfaced to a computer.

The ion extraction and transport system [12] was used to obtain information about the distribution of ion charge states within the EBIT. Briefly, the trap was emptied on-axis, allowing the ions to be extracted from the EBIT along the magnetic field lines, after which a series of electrostatic elements focused and aligned the ion beam before sending it through a charge to mass ratio analyzing magnet. The charge states were separated using the magnet and a detector counted the number of ions transported through the magnet for a particular value of the magnetic field. By successively stepping the magnetic field and emptying the trap, a plot of the relative populations of the charge states present in the trap was obtained.

III. DATA

Figure 1 shows a Kr spectrum taken at a drift tube voltage of 10 kV. The upper, middle, and lower drift tubes floating voltages were set at 450 V, 0 V, and 500 V, respectively. The entrance and exit slits of the monochromator were set to 500 μm. The data shown took about 2 hours to accumulate and are the sum of seven spectral scans, each one with a different time between unloading the trap, ranging from 5 ms to 60 ms. We identify the peak at 384 nm to be the $3s^2 3p^2\,{}^3P_1 \leftarrow {}^3P_2$ transition in Kr XXIII and the peak at 346.47 nm to be the $3s^2 3p^3\,{}^2D_{3/2} \leftarrow {}^2D_{5/2}$ transition in Kr XXII. Most of the remaining spectrum, except the peak at 402.58 nm, can be attributed to Kr II and Kr III. The 384-nm line was predicted to be at 383.2(40) by Kaufman and Sugar [9] and observed first by Roberts *et al.* [20] in a tokamak. The line at 346.47 nm has not been previously observed but was predicted [9] to be at 344.6(30) nm. Only one other $M1$ line is predicted in Ref. [9] for the range of 300 nm to 400 nm, a line at 313.4 nm which was not observed.

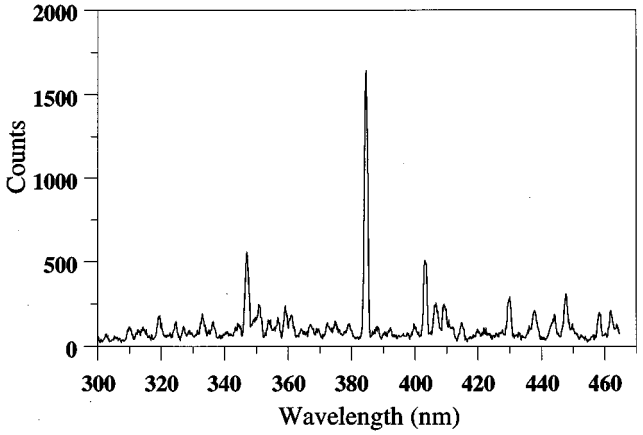

FIG. 1. Survey spectrum from 300 nm to 460 nm taken during Kr gas injection at an electron beam energy of $\sim$10 keV, and 500-μm slits.

Extracted ion data are shown in Fig. 2, where ion beam intensity is plotted as a function of analyzing magnetic field. The plot shows the different charge states present in the trap as well as their relative populations. The peaks corresponding to Kr XXIII and Kr XXII are indicated with arrows in the plot. Weaker peaks near the main peaks indicate the presence of less abundant Kr isotopes in the trap. The electron beam energy used during extraction (10 keV) did not maximize the relative populations of these charge states but allowed us to increase the electron beam current and thus the absolute signal of these charge states compared to that obtained at lower currents. This particular plot was obtained while emptying the trap every 40 ms.

Another way of aiding charge state identification is to compare the temporal buildup of the individual line intensities. Time resolved data (Fig. 3) were taken for the 384-nm (Kr XXIII), 346.47-nm (Kr XXII), 402.58-nm, and 429.3-nm (Kr II) lines with an electron beam energy of approximately 5 kV, a current of 84 mA, and a pressure of 2×10^{-3} Pa in the gas injection system. Data corresponding to different transitions have been normalized so that all the plots reach the same equilibrium value for long times. The plots show the trap being emptied near the 20-ms mark. The 346.47-nm line shows a time evolution consistent with our charge state iden-

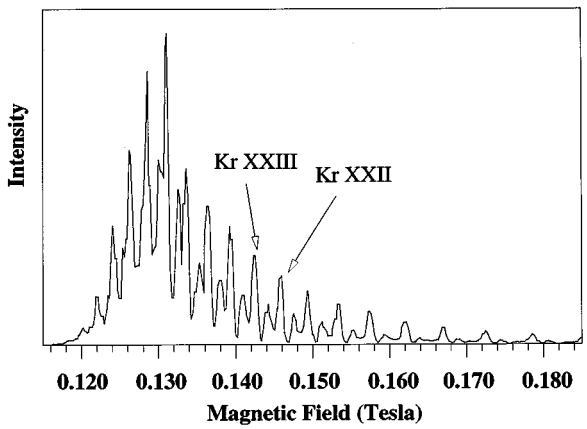

FIG. 2. Extracted ion beam intensity vs magnetic field. The two arrows show the peaks corresponding to Kr XXIII and Kr XXII.

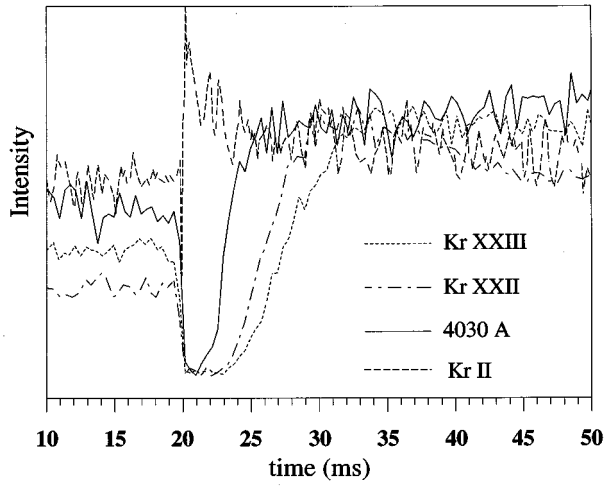

FIG. 3. Time resolved spectral intensity of various lines. The trap is being emptied near the 20-ms mark.

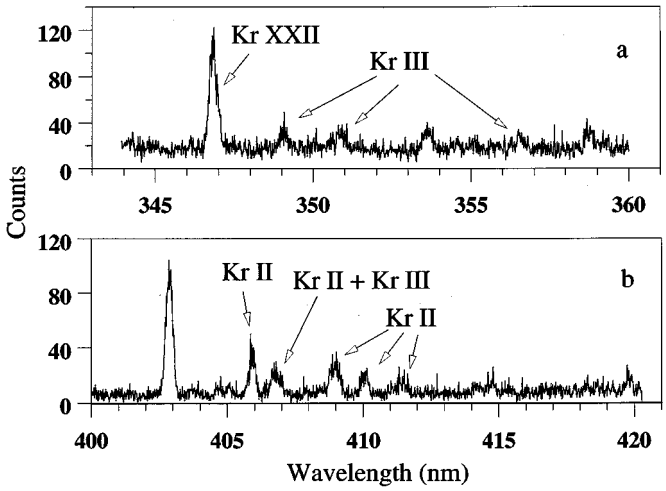

FIG. 4. Spectral scans taken with 100-μm entrance and exit slits. Peaks are labeled with their respective charge state identification.

tification (Kr XXII), i.e., it rises just before the Kr XXIII line, as would be expected for a sequential ionization process such as electron impact inside the EBIT. The data also suggest that the unidentified line at 402.58 nm belongs to a charge state lower than Kr XXII. Using the tabulated energy levels of Kr [11] we searched for possible $M1$ transitions arising from the ground state term and found no suitable candidate for this unidentified line. The lack of energy levels for the $3p^6 3d^n$ $(n=2$ to $8)$ charge states of Kr makes the identification difficult. A possible candidate for this line was proposed in a similar spectroscopic study [16] carried out in a partially overlapping spectral region by the Livermore group using their EBIT. The identification proposed by that group is the magnetic dipole $(M1)$ $2p^5 3d\,^3P_1 \leftarrow {}^3P_2$ transition in Kr XIX. The upper level of this transition $({}^3P_2)$ is low enough to be easily populated by direct electron impact excitation or through cascading, and because of its angular momentum cannot decay to the ground state $(2p^6)$ via $E1$. Calculated energy levels [17] as well as solar coronal identification of lines [18] arising from the first excited configuration of the Ar isoelectronic sequence exist in the literature but only up to Ar-like Ni. The extrapolated energy difference to Kr XIX is in reasonable agreement with our measurement but further observations along the isoelectronic sequence are required for a definite identification. The time behavior of the Kr II line is consistent with a fast rise of this low charge state right after the middle drift tube voltage is raised and lowered.

Scans of the lines at 346.47 nm and 402.58 nm were taken with an electron beam energy of $\sim$10 kV, a current of 141 mA, and 100-μm entrance and exit slits. Figure 4 shows two such scans, both of which also show smaller features at lower wavelengths that we identify as Kr II and Kr III. We use these *in situ* lines for wavelength calibrations instead of lines from a conventional stationary light source to eliminate the uncertainty introduced by the wavelength shifts due to the placement of the stationary source outside the EBIT. In order to use these lower charge state lines for wavelength calibration, the influence of the magnetic and electric field on their transition wavelength should be considered. The effect of the magnetic field (Zeeman effect) is to remove the m degeneracy. Considering that only transitions with $|\Delta m|=1$ are allowed for $E1$ and $M1$ transitions, we estimate that the magnetic components of the lines shift by approximately 0.027 nm and 0.075 nm (3 cm^{-1}) for lines at 300 nm and 500 nm, respectively. These shifts are symmetric so there is no net shift but an overall broadening of the line [19]. We estimate this broadening due to the Zeeman effect to be about 6 cm^{-1}. To consider the effects of the electric field (Stark effect) inside the EBIT we estimate the electron density to be $\sim 4\times 10^{12}$ cm^{-3} $(7\times 10^{-1}$ C/m$^3)$ and conclude that the maximum macroscopic electric field from the electron beam is $\sim 1\times 10^3$ kV/m. The actual total electric field will be smaller than this, depending on the degree of neutralization of the trap. Assuming 20% neutralization of the trap, we obtain a value of 8×10^2 kV/m. Another possible contribution to the electric field comes from the voltage differential between the central drift tube and the endcaps. Assuming a potential difference of about 400 V in a distance of about one-tenth of the trap length (0.2 cm), we obtain an electric field of about 200 kV/m in the small region of the voltage drop. This is smaller than the electron beam contribution. The Stark effect does not produce a shift in first order (except for hydrogen), so in general the shifts are proportional to the square of the electric field. The Kr lines used for calibration were $s^2p^4(^1D)5s \leftarrow s^2p^4(^1D)5p$ and $s^2p^4(^3P)5s \leftarrow s^2p^4(^3P)5p$ for Kr II, and $s^2p^3(^2D)4d - (^2D)5p$ and $s^2p^3(^4S)5s - (^4S)5p$ for Kr III. Di Rocco *et al.* [21] have measured line shifts due to the microscopic Stark effect in similar lines of Kr II and Kr III in a pinched

TABLE I. Different contributions to the uncertainties. All values quoted in nanometers. The final uncertainties (1-σ level) are computed by combining the individual uncertainties in quadrature.

Line (nm)	Calibration/Fitting	Reproducibility	Uncertainty
346.47	0.05	0.04	0.06
402.58	0.02	0.04	0.05

discharge. They estimate the electric field to be 5×10^4 kV/m. All the shifts are smaller than 1 cm^{-1}. Using this value and the fact that the shifts are proportional to the square of the electric field, we estimate negligible shifts due to the Stark effect in the EBIT for low charge states of Kr.

By using the low charge states of Kr as wavelength calibration lines, we obtain 346.47(6) nm for the Kr XXII line and 402.58(5) nm for the unidentified line. The quoted wavelengths are measured in air and the uncertainties are the result of adding in quadrature the uncertainties from the fits and reproducibility at the one standard deviation uncertainty level. Table I shows the different contributions to the final uncertainties.

In conclusion, we have shown how the EBIT is an important source not only of $M1$ lines for highly charged ions, but also for lines in moderately charged ions as well, even when the electron beam energy is well beyond that required to optimize the production of the moderately charged ions. A previously unobserved $M1$ line in Kr XXII was measured. The usefulness of the ion extraction system and time resolved data as charge state identification tools was also shown.

ACKNOWLEDGMENTS

We would like to thank E. Träbert for helpful discussions.

[1] C. A. Morgan, F. G. Serpa, E. Takács, E. S. Meyer, J. D. Gillaspy, J. Sugar, J. R. Roberts, C. M. Brown, and U. Feldman, Phys. Rev. Lett. **74**, 1716 (1995).
[2] F. G. Serpa, E. S. Meyer, C. A. Morgan, J. D. Gillaspy, J. Sugar, J. R. Roberts, C. M. Brown, and U. Feldman, Phys. Rev. A **53**, 2220 (1996).
[3] S. Suckewer and E. Hinnov, Phys. Rev. Lett. **41**, 756 (1978).
[4] R. U. Datla, J. R. Roberts, W. L. Rowan, and J. B. Mann, Phys. Rev. A **34**, 4751 (1986).
[5] K. H. Burrell, R. J. Groebner, N. H. Brooks, and L. Rottler, Phys. Rev. A **29**, 1343 (1984).
[6] B. Edlén, Ark. Mat. Astr. Fys. **28**B, 1 (1941).
[7] B. Edlén, Z. Astrophys. **22**, 30 (1942).
[8] U. Feldman, P. Indelicato, and J. Sugar, J. Opt. Soc. Am. B **8**, 3 (1991).
[9] V. Kaufman and J. Sugar, J. Phys. Chem. Ref. Data **15**, 1 (1986).
[10] T. Shirai, K. Okazaki, and J. Sugar, J. Phys. Chem. Ref. Data **24**, 1577 (1995).
[11] J. Sugar and A. Musgrove, J. Phys. Chem. Ref. Data **20**, 859 (1991).
[12] A. I. Pikin, C. A. Morgan, E. W. Bell, L. P. Ratliff, D. A. Church, and J. D. Gillaspy, Rev. Sci. Instrum. **67**, 2528 (1996).
[13] J. D. Gillaspy, J. R. Roberts, C. M. Brown, and U. Feldman, in *VIth International Conference on the Physics of Highly Charged Ions*, edited by P. Richard, M. Stockli, C. L. Cocke, and C. D. Lin, AIP Conf. Proc. No. 274 (AIP, New York, 1992), p. 682.
[14] R. E. Marrs, P. Beiersdorfer, and D. Schneider, Phys. Today, **47**(10), 27 (1994).
[15] J. D. Gillaspy, Y. Aglitskiy, E. W. Bell, C. M. Brown, C. T. Chantler, R. D. Deslattes, U. Feldman, L. T. Hudson, J. M. Laming, E. S. Meyer, C. A. Morgan, A. I. Pikin, J. R. Roberts, L. P. Ratliff, F. G. Serpa, and E. Takács, Phys. Scr. **T59**, 392 (1995).
[16] J. R. Crespo López–Urrutia, P. Beiersdorfer, K. Widmann, and V. Decaux, in *10th APS Topical Conference on Atomic Processes in Plasmas, Program and Abstracts, A5* (Lawrence Livermore National Laboratory, San Francisco, 1996).
[17] W. J. Wagner and L. L. House, Astrophys. J. **166**, 683 (1971).
[18] L. Å. Svensson, J. O. Ekberg, and B. Edlén, Solar Phys. **34**, 173 (1974).
[19] I. I. Sobelman, *Atomic Spectra and Radiative Transitions*, 2nd ed. (Springer Verlag, Berlin, 1992).
[20] J. R. Roberts, T. L. Pittman, J. Sugar, V. Kaufman, and W. L. Rowan, Phys. Rev. A **35**, 2591 (1987).
[21] H. O. Di Rocco, G. Bertuccelli, J. Reyna Almandos, F. Bredice, and M. Gallardo, J. Quant. Spectrosc. Radiat. Trans. **41**, 161 (1989).